Virchows Archiv (1995) 426:257–266

ORIGINAL ARTICLE

Petter C. Endresen · Jørgen Fandrem · Tor Jac Eide
Jarle Aarbakke

Morphological modifications of apoptosis in HL-60 cells: effects of homocysteine and cytochalasins on apoptosis initiated by 3-deazaadenosine

Received: 31 May 1994 / Accepted: 21 October 1994

Abstract Using electron microscopy, confocal laser scanning microscopy and measurements of intact DNA we have studied the morphology and DNA degradation of human leukaemia HL-60 cells undergoing drug initiated apoptosis. Apoptosis was initiated by 100 μM 3-deazaadenosine (c^3Ado), 25 μM c^3Ado plus 1 mM homocysteine thiolactone (Hcy) and 100 μM c^3Ado plus 5 μg/ml cytochalasin B (CB). Two different phenotypes of apoptotic cells (APC), blebbed and non-blebbed, were present in the cultures. Blebbed APC dominated in cultures exposed to c^3Ado, whereas most APC in cultures treated with c^3Ado plus Hcy and all the APC in cultures treated with c^3Ado plus CB displayed a non-blebbed phenotype. A more pronounced reduction of the chromatin/cytoplasm ratio, lower volume fractions of uncondensed chromatin and higher volume fractions of highly condensed chromatin (micronuclei) were found in cultures exposed to c^3Ado and c^3Ado plus Hcy when compared with cultures exposed to c^3Ado plus CB. A partial inhibition of c^3Ado apoptosis by CB was confirmed by measurements of intact DNA. The inhibitory effect of CB was not reproducible by CE, indicating that CB exerts its effect by an actin independent mechanism. Both blebbed and non-blebbed APC displayed nuclear fragmentation, segregation of organelles and cytoplasmic vesiculation, suggesting that the differences between the phenotypes were restricted to the cytoplasmic membrane. We were not able to demonstrate the presence of F-actin by fluorescein isothiocyanate-phalloidin staining in blebbed APC nor in non-blebbed APC in cultures treated with c^3Ado plus Hcy. Non-blebbed APC in cultures treated with c^3Ado plus CB displayed foci of F-actin at the internal part of the cytoplasmic membrane. This suggests that F-actin is preserved by the mechanism by which CB inhibits blebbing, and may indicate that blebbing of the cytoplasmic membrane during apoptosis is associated with F-actin deficiency rather than a result of actin-myosin interactions.

Key words Apoptosis · 3-Deazaadenosine · Homocysteine · Cytochalasins · Blebbing

P. C. Endresen (✉) · J. Aarbakke
Department of Pharmacology, Institute of Medical Biology, University of Tromsø, MH-Breivika, N-9037 Tromsø, Norway

J. Fandrem
Department of Experimental Pathology, Institute of Medical Biology, University of Tromsø, Tromsø, Norway

T. J. Eide
Department of Morphology, Institute of Medical Biology, University of Tromsø, Tromsø, Norway

Introduction

The morphological transformation of apoptotic death is characterized by cellular condensation and fragmentation processes [1, 30, 57]. Variations in the morphology of apoptosis among cell types have been reported [6], and the type of structural apoptotic changes may depend upon the stimulus leading to apoptosis [22]. In the human promyelocytic HL-60 cell line apoptosis is characterized by chromatin condensation, nuclear fragmentation and endonucleolytic DNA degradation. These changes give rise to apoptotic cells (APC) containing micronuclear particles of different size and density. A pronounced blebbing of the cytoplasmic membrane parallels the nuclear changes in HL-60 cell apoptosis. The mechanism(s) underlying the blebbing process remain uncertain. Actin polymerization [11], disrupture of the cytoskeleton [43] and perturbations of the phosphorylation-dephosphorylation equilibria of intermediate filaments and microfilament associated proteins [16] have been associated with membrane blebbing in different experimental systems.

We have previously reported that 50–100 μM of the adenosine analogue 3-deazaadenosine (c^3Ado) initiates apoptosis in HL-60 cells [14]. Furthermore, we have demonstrated that addition of homocysteine thiolactone (Hcy) to c^3Ado exposed cells modifies apoptotic death in this cell line in two different ways. Firstly, Hcy potentiates the ability of c^3Ado to initiate apoptosis, as addition

of Hcy leads to apoptosis also at lower concentrations (5–25 μM) of c^3Ado [15]. Secondly, addition of Hcy modifies the morphology of c^3Ado apoptosis by inhibiting blebbing of the cytoplasmic membrane and the formation of apoptotic bodies (APB) [14, 15].

The mechanism by which c^3Ado initiates apoptosis is not known. However, c^3Ado interacts both as inhibitor and substrate with S-adenosylhomocysteine hydrolase (AdoHcyase; EC 3.3.1.1.) causing subsequent perturbation of transmethylation reactions [8, 54].

Cytochalasins affect a variety of motility related cellular functions as locomotion, endocytosis, and cytokinesis by interacting with microfilaments [10, 58]. In contrast to other cytochalasins, cytochalasin B (CB) also affects glucose transport at site I as defined by Rampal et al. [45; also 7]. In addition, several non motility related effects of CB are demonstrated including mitogen stimulation [33] and elevation of intracellular calcium levels [20, 52]. CB and cytochalsin E (CE) have been shown to prevent formation of APB without affecting DNA degradation in HL-60 cells undergoing apoptosis [11]. However, in another experimental system CB and CE initiated apoptotic DNA-fragmentation [31].

The present study was undertaken to investigate the morphological differences between HL-60 cells treated with 100 μM c^3Ado and 25 μM c^3Ado plus 1 mM Hcy at the ultrastructural level. Since blebbing of APC and formation of APB might involve actin polymerization [11], we compared the morphological features of HL-60 cells treated with c^3Ado and c^3Ado plus Hcy with that of c^3Ado and 5 μg/ml of a known inhibitor of actin polymerization, CB. A stereological method was applied in order to quantify the relations between the volumes of different cell components, and fluorescein isothiocyanate (FITC)-phallodin staining was used to visualize actin filaments.

Materials and methods

c^3Ado was obtained from Southern Research Institute (Birmingham, Ala., USA). Hcy, CB and CE, FITC-phalloidin, and RNase were purchased from Sigma Chemical Company (St. Louis, Mo., USA). CB and CE were freshly dissolved in dimethyl sulfoxide at 10 mM and further diluted in medium prior to each experiment. Propidium iodide (PI) was from Molecular Probes, (Eugene, Ore., USA) and tritiated thymidine from ICN Radiochemicals (Irvine, Calif., USA).

HL-60 cells were maintained in RPMI 1640 supplemented with 10% heat inactivated horse serum in a fully humidified atmosphere of 5% carbondioxide at 37° C. Suspensions of cells were adjusted to concentrations of early logarithmic growth. Drugs dissolved in RPMI 1640 (ten-fold final concentration) were added, and cultures were harvested after 2, 4, 6, 8, 10 and 12 h and processed for analysis. Since 25 μM c^3Ado plus 1 mM Hcy alters the morphology of c^3Ado apoptosis and at the same time is comparable with 100 μM c^3Ado with respect to potency of initiating apoptosis [15], these concentrations were chosen for our study. Cell counts were determined by a haemocytometer.

At the end of incubation cells were fixed by addition of an equal volume of McDowell fixative [40] directly to the culture flasks. After 1 h storage at 4° C the medium was removed after centrifugation at 200 *g*, and the cells resuspended in 1 ml McDowell fixative. Fixed cells were stored at 4° C. The samples were further prepared for transmission electron microscopy (TEM) and scanning electron microscopy (SEM) according to standard methods.

A stereological method was used to quantify the relations between the volumes of different cell components. Micrographs (×3,000) were taken from the upper left corner of every second grid square in decoded preparations. Photomicrograph positives were covered by a counting frame, and the different volume fractions were estimated by simple point counting [25]. Five micrographs were analysed at each time interval. The total number of counts varied between 252 and 419. The following volume fractions (Vv) were estimated: Vv (cytoplasm/the whole cell), Vv (uncondensed chromatin/the whole cell), Vv (partially condensed chromatin/the whole cell), Vv (micronuclei/the whole cell), Vv (vesicles/the whole cell). The degree of condensation of partly condensed chromatin corresponded to that displayed by nucleoli in control cells. Micronuclei were defined as separate different sized particles of highly condensed chromatin with a smooth boundary to the surrounding cytoplasm. The chromatin/cytoplasm ratio were determined by comparing the sum of Vv (uncondensed chromatin/the whole cell), Vv (partially condensed chromatin/the whole cell), Vv (micronuclei/the whole cell) to the sum of Vv (cytoplasm/the whole cell) and Vv (vesicles/the whole cell).

The surface structures of treated and control cells were evaluated in decoded SEM preparations. The number of smooth surfaced cells (cells lacking pseudopodium covering), non-blebbed and blebbed, were evaluated directly on the EM monitor at a magnification of ×3,500. Only cells with a completely smooth surface were categorized as smooth surfaced cells. One hundred cells were counted in each preparation.

The relative amount of intact DNA was estimated as described by Matzinger [39]. Briefly, cells were labelled with 5 μCi/ml tritiated thymidine for 5 h, washed once and resuspended in fresh medium. After drug exposure cells were harvested onto fibreglass filters retaining intact DNA only. Activity was measured in a Matrix 96 direct beta counter (Packard Instrument Company, Meriden, Conn., USA).

For fluorescence microscopy, at the end of incubation, cells were fixed by addition of an equal volume of 3.7% formaldehyde directly to the culture flasks [56]. After 1 h storage at 4° C the medium was removed after centrifugation at 200 *g*, and the cells resuspended in 1 ml 3.7% formaldehyde and stored at 4° C. At the time of evaluation the cells were washed once in phosphate-buffered saline (PBS) containing 0.1% Triton, washed again in PBS and treated with 0.1% sodium borohydride in PBS pH 8 for 30 min to reduce autofluorescence. F-actin was stained for 1 h by 50 μg/ml FITC-phalloidin. Post staining the cells were washed twice in PBS, and finally DNA was stained by 10 μg/ml PI supplemented with 100 μg/ml RNase. The anti-fading agent DABCO (0.1 g/ml) was added prior to evaluation. Wet preparations of stained cells were examined in a Leica Fluovert FU confocal laser scanning microscope with argon/krypton laser excitation at 488 and 568 nm. Green fluorescence (F-actin) was detected with a 515–545 band pass filter and red fluorescence (DNA) with a 580 nm long pass filter. Ten sections of each preparation were scanned. Photomicrographs were taken with Fujichrome 64 T type film.

Results

Ultra structure evaluation by TEM

Whereas control cells displayed large and distinct nucleoli (Fig 1), smaller nucleoli or their absence was observed in the nuclei of cells treated with c^3Ado, c^3Ado plus Hcy and c^3Ado plus CB for 2 h. In addition some

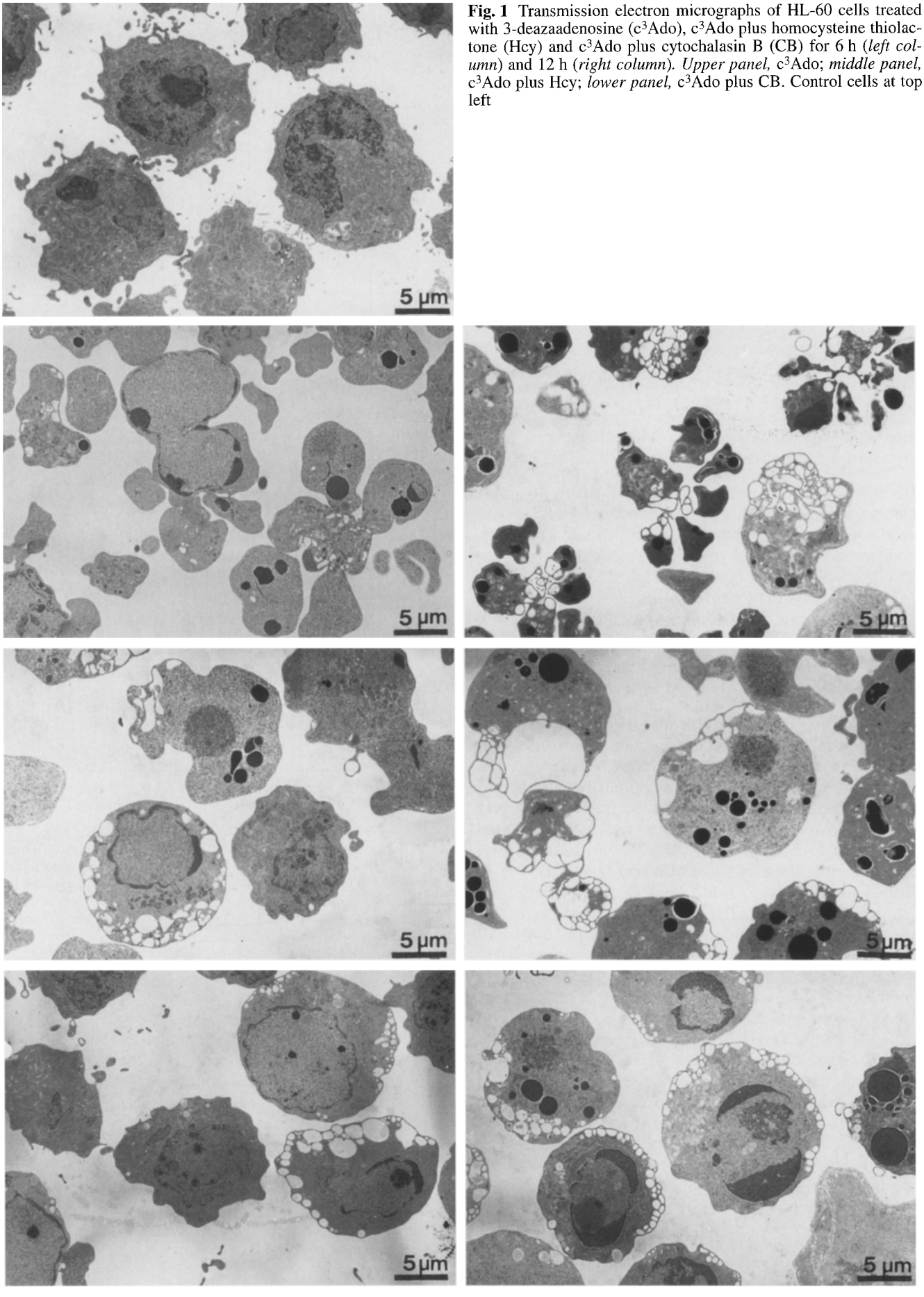

Fig. 1 Transmission electron micrographs of HL-60 cells treated with 3-deazaadenosine (c^3Ado), c^3Ado plus homocysteine thiolactone (Hcy) and c^3Ado plus cytochalasin B (CB) for 6 h (*left column*) and 12 h (*right column*). *Upper panel,* c^3Ado; *middle panel,* c^3Ado plus Hcy; *lower panel,* c^3Ado plus CB. Control cells at top left

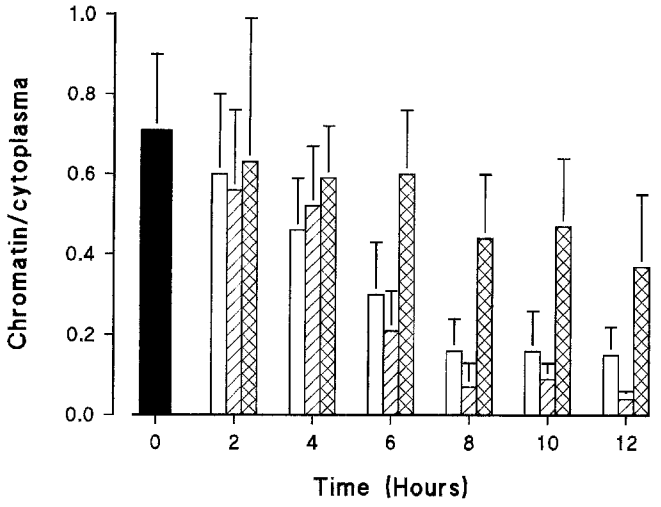

Fig. 2 Time course relationship of the chromatin/cytoplasm ratio of HL-60 cells treated with c^3Ado (*open bars*), c^3Ado plus Hcy (*/bars*) and c^3Ado plus CB (*X bars*). The ratio was estimated as described in the methods. Control cells, *solid bar.* The results are means, error bars indicate standard deviation (SD; n=5).

cells in cultures exposed to c^3Ado and c^3Ado plus Hcy demonstrated small patches of condensed chromatin. After 4 h this was evident in all drug treated cultures, being more pronounced in cultures treated with c^3Ado and c^3Ado plus Hcy. Typical nuclear features of early apoptosis, that is different sized patches of partly condensed chromatin located centrally and crescents of partly condensed chromatin at the nuclear margins, were distinct in cultures treated with c^3Ado and c^3Ado plus Hcy for 6 h (Fig 1). A gradual reduction of the chromatin/cytoplasm ratio in cultures exposed to c^3Ado and c^3Ado plus Hcy reflected ongoing nuclear condensation (Fig 2). In cultures exposed to c^3Ado plus CB there was a more moderate reduction in the chromatin/cytoplasm ratio (Fig. 2). An increasing number of APC, displaying nuclei completely transformed into several micronuclei, were present in cultures treated with c^3Ado and c^3Ado plus Hcy for 6–12 h (Fig 1). APC with micronuclei were first evident after 8 h in cultures treated with c^3Ado plus CB. The different Vv of uncondensed chromatin, partly condensed chromatin and micronuclei are demonstrated in Figure 3. A small number of cells with uncondensed chromatin were present in cultures treated with c^3Ado up to 12 h (Fig 3, *upper panel*), whereas all the chromatin in cells treated with c^3Ado plus Hcy were converted into micronuclei (Fig 3, *middle panel*). In cultures treated with c^3Ado plus CB large volumes of uncondensed chromatin were present up to 12 h (Fig 3, *lower panel*). APC in all treated cultures demonstrated typical organelle segregation and cytoplasmic vesiculation (Figs. 1, 4). Vesicles were located close to the cytoplasmic membrane in non-blebbed APC, and fusions between vesicles and the cytoplasmic membrane were observed. No apoptotic changes were observed in cultures treated with 1 mM Hcy or 5 μg/ml CB alone (data not shown).

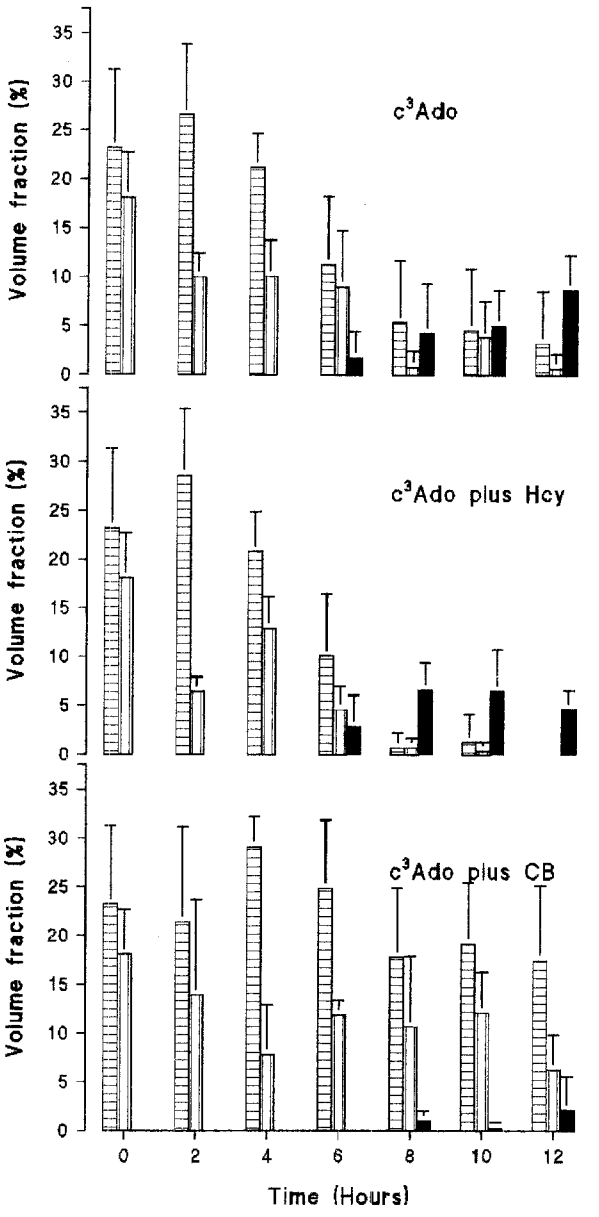

Fig. 3 Time course relationship of the volume fraction (Vv) of uncondensed chromatin (– *bars*), partly condensed chromatin (| *bars*) and micronuclei (*solid bars*) of HL-60 cells exposed to c^3Ado (*upper panel*), c^3Ado plus Hcy (*middle panel*) and c^3Ado plus CB (*lower panel*). The results are means, error bars indicate SD (n=5)

DNA fragmentation

The finding of higher Vv of uncondensed chromatin in cultures treated with c^3Ado plus CB compared to that found in cultures treated with c^3Ado and c^3Ado plus Hcy, was further investigated by measurements of intact DNA. A marked decline in intact DNA after 4–6 h was evident in cultures exposed to c^3Ado and c^3Ado plus Hcy (Fig 5, *upper panel*). A gradual reduction to 66.0% intact DNA after 12 h was observed in cultures exposed to c^3Ado plus CB (Fig 5, *lower panel*). To examine whether the inhibitory effect of CB on DNA degradation was

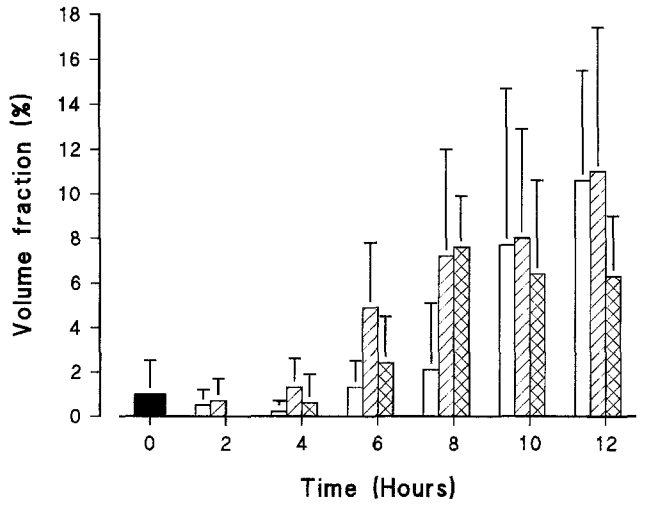

Fig. 4 Time course relationship of the Vv of vesicles in cultures treated with c^3Ado (*open bars*), c^3Ado plus Hcy (*/ bars*) and c^3Ado plus CB (*X bars*). Control cells, *solid bar.* The results are means, error bars indicate SD (n=5)

common for all cytochalasins, measurements of intact DNA were conducted in cultures exposed to c^3Ado plus 5 µg/ml CE (Fig 5, *lower panel*). In contrast to CB, CE increased DNA degradation in c^3Ado apoptosis. No DNA degradation was observed in cultures exposed to CB and CE alone (data not shown).

Ultra structure evaluation by SEM

Compared with controls, all treated cells showed an altered pseudopodium covering by SEM. After 4 h cells with a completely smooth surface were observed. Smooth surfaced cells displayed either a blebbed phenotype or a non-blebbed phenotype (Fig 6). Cells treated with CB only exhibited a polarized shape and often longer and broader pseudopodia covering a limited area of the cell surface. Whereas the percentage of smooth surface cells increased from 9%–90% in cultures treated with c^3Ado and from 16%–99% in cultures treated with c^3Ado plus Hcy for 4–12 h, the number of smooth surfaced cells in cultures exposed to c^3Ado plus CB did not exceed 38% (Fig 7). In cultures treated with c^3Ado a majority of the smooth surfaced cells were blebbed, whereas no blebbed cells were observed in cultures treated with c^3Ado plus CB (Fig 7). A few cells with a complete smooth surface were observed in cultures treated with CB alone for 12 h (data not shown).

F-actin distribution

To investigate F-actin distribution in APC, F-actin and DNA were stained with FITC-phalloidin and PI, respectively. As demonstrated in Figure 8, apoptotic nuclei were evident in both blebbed and non-blebbed cells (panels C and D). When compared with control cells (panel A) and

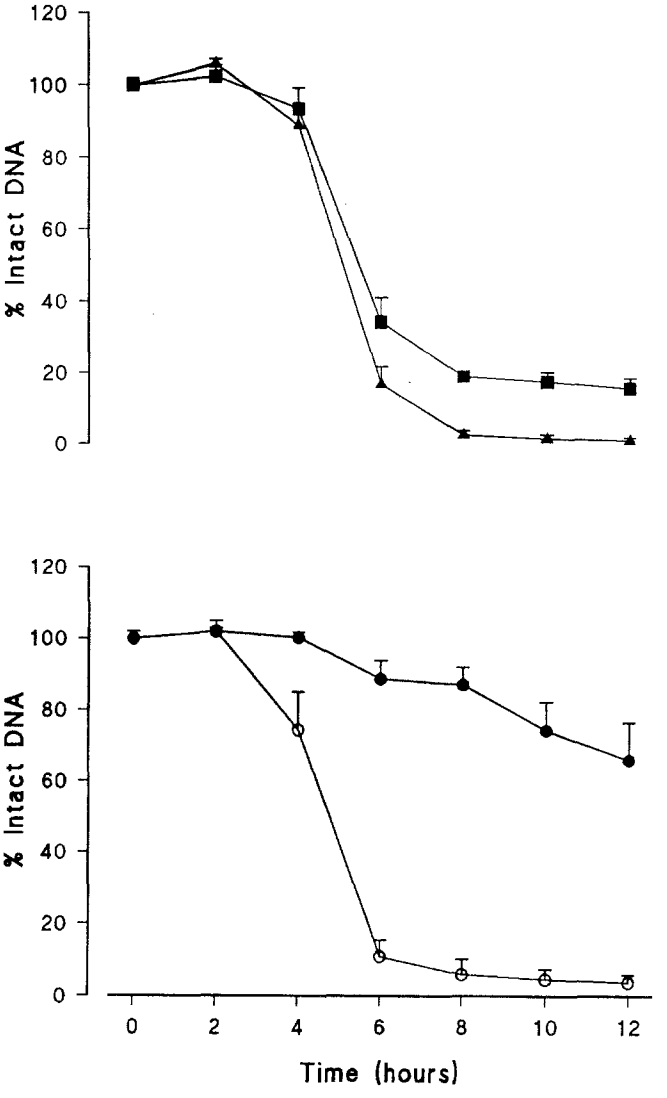

Fig. 5 Time course relationship of intact DNA in cultures treated with c^3Ado (■) and c^3Ado plus Hcy (▲) (*upper panel*) and c^3Ado plus CB (●) and c^3Ado plus cytochlasin E (CE; ○) (*lower panel*). Data as percentage of intact DNA of that of control cells at each time interval. The results are means, error bars indicate SD (n=3)

cells treated with CB (panel B), the blebbed APC in cultures treated with c^3Ado and non-blebbed APC in cultures treated with c^3Ado plus Hcy demonstrated a total loss of the green fluorescent component of the cytoplasmic membrane and the cell surface (panels C and D). This loss of surface F-actin propably reflects the loss of pseudopodium covering observed by SEM. We were unable to detect any distinct green fluorescence in the cytoplasm of blebbed nor non-blebbed APC in these cultures. Most cells treated with c^3Ado plus CB displayed intact nuclei and F-actin distribution comparable with that of cells treated with CB only (panel E). Some cells in these cultures demonstrated nuclear margins or spheres within the nuclei with a stronger red fluorescence corresponding to early apoptosis. A loss of the green fluorescent component of the cell surface was also displayed by these cells.

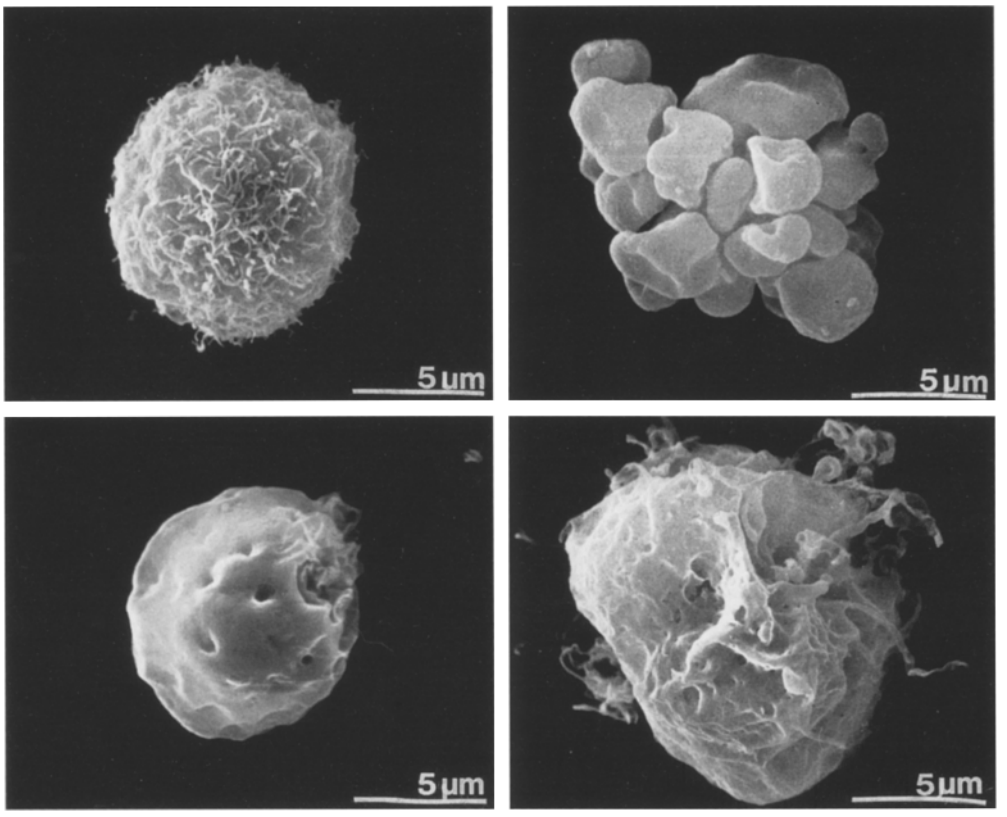

Fig. 6 Scanning electron micrographs of HL-60 cells treated with c^3Ado, c^3Ado plus Hcy and c^3Ado plus CB for 8 h. *Upper left,* control cell; *upper right,* blebbed APC from culture exposed to c^3Ado; *lower left,* non-blebbed APC from culture exposed to c^3Ado plus Hcy; *lower right,* cell with altered pseudopodial covering from culture exposed to c^3Ado plus CB. Note the larger diameter of the blebbed APC compared with the non-blebbed APC

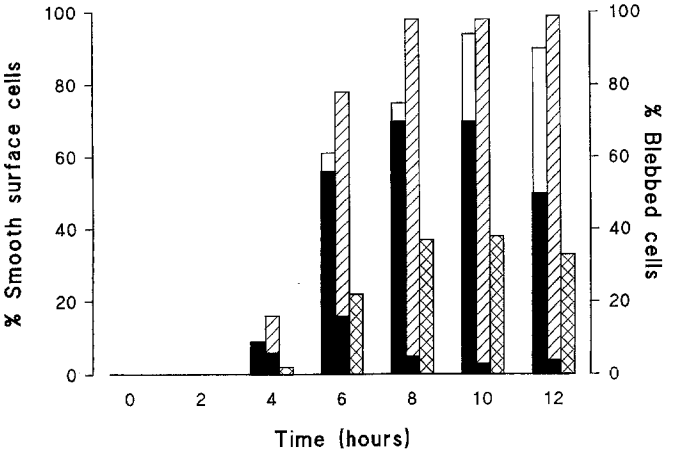

Fig. 7 Time course relationship of the percentage of smooth surfaced cells in cultures exposed to c^3Ado (*open bars*), c^3Ado plus Hcy (*/ bars*) and c^3Ado plus CB (*X bars*). The fraction of blebbed APC (*solid bars*) is superimposed on each bar

However, in contrast with APC in cultures treated with c^3Ado and c^3Ado plus Hcy, these cells often demonstrated foci of green fluorescence at the internal part of the cytoplasmic membrane (panel E).

Discussion

We present a comparison of the morphological features of HL-60 cells undergoing apoptosis due to treatment with c^3Ado, c^3Ado plus Hcy and c^3Ado plus CB. Our data suggest the presence of two different phenotypes of APC, blebbed and non-blebbed, and demonstrate that CB partly inhibits c^3Ado apoptosis.

Cell shrinkage and nuclear condensation and fragmentation are well established criteria of apoptosis [57]. Classical apoptosis also displays segregation of intact organelles, vesiculation, loss of cell surface structures, blebbing of the cell surface and finally disintegration of the whole cell into APB [1, 9, 30]. In the present study nuclear condensation in the form of small patches of partly condensed chromatin was evident in some cells in cultures exposed to c^3Ado and c^3Ado plus Hcy already after 2 h. We did not observe loss of intact DNA until 4 h in these cultures. Arends et al. [2] have suggested that chromatin condensation in apoptosis actually reflects endonuclease activity. However, several reports have demonstrated that chromatin condensation and DNA fragmentation are separate processes [34, 42, 49]. The present data suggest that chromatin condensation starts prior to DNA degradation in HL-60 cells undergoing apoptosis.

In cultures exposed to both c^3Ado and c^3Ado plus Hcy for 2–12 h there was increasing chromatin condensation and nuclear fragmentation reflected by a reduction in the chromatin/cytoplasm ratio, a decrease in the Vv of uncondensed chromatin and an increase in the Vv of micronuclei. The fact that no uncondensed chromatin was left in cells exposed to c^3Ado plus Hcy, and that the chromatin/cytoplasm ratio of c^3Ado plus Hcy treated

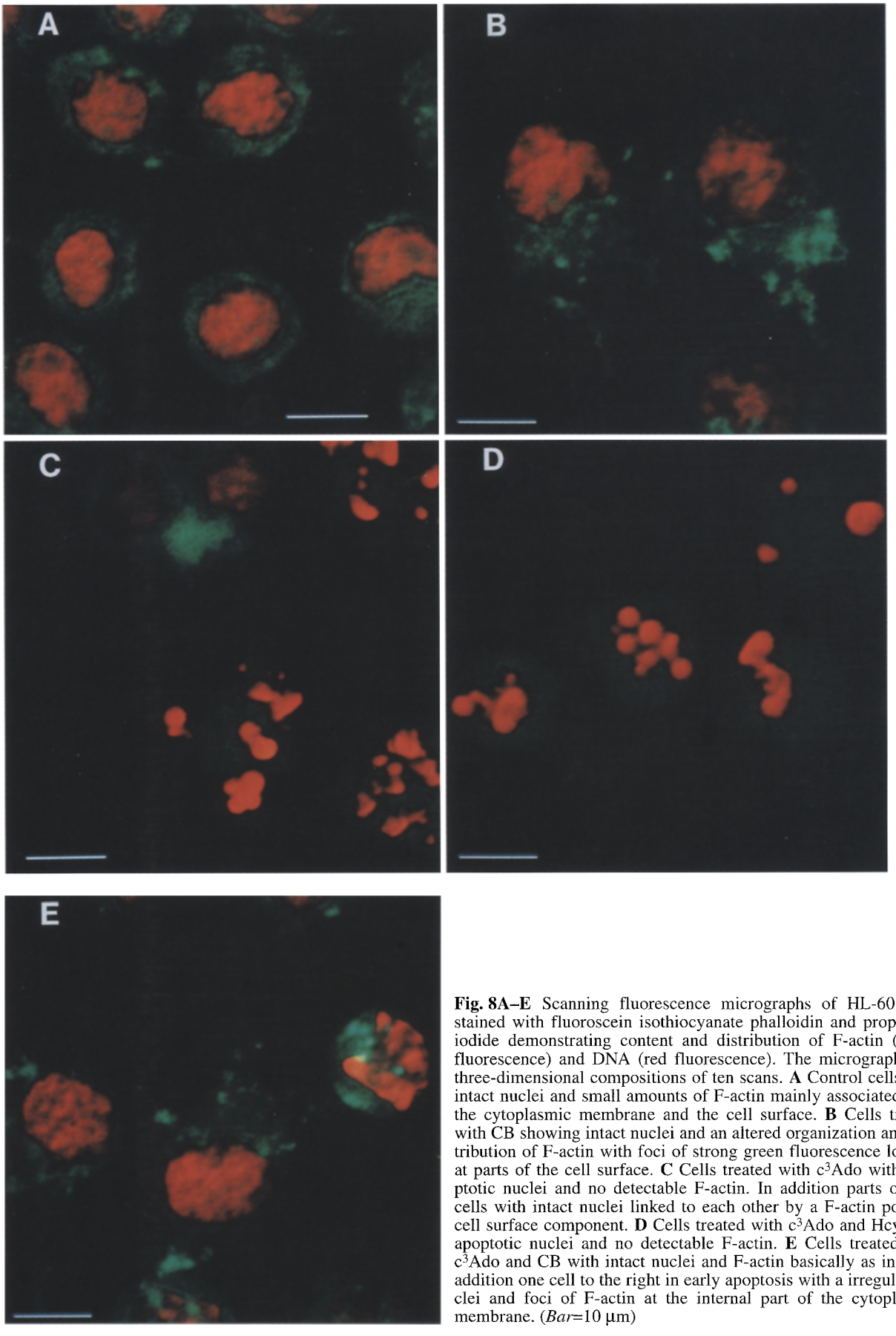

Fig. 8A–E Scanning fluorescence micrographs of HL-60 cells stained with fluoroscein isothiocyanate phalloidin and propidium iodide demonstrating content and distribution of F-actin (green fluorescence) and DNA (red fluorescence). The micrographs are three-dimensional compositions of ten scans. **A** Control cells with intact nuclei and small amounts of F-actin mainly associated with the cytoplasmic membrane and the cell surface. **B** Cells treated with CB showing intact nuclei and an altered organization and distribution of F-actin with foci of strong green fluorescence located at parts of the cell surface. **C** Cells treated with c^3Ado with apoptotic nuclei and no detectable F-actin. In addition parts of two cells with intact nuclei linked to each other by a F-actin positive cell surface component. **D** Cells treated with c^3Ado and Hcy with apoptotic nuclei and no detectable F-actin. **E** Cells treated with c^3Ado and CB with intact nuclei and F-actin basically as in **B**. In addition one cell to the right in early apoptosis with a irregular nuclei and foci of F-actin at the internal part of the cytoplasmic membrane. (*Bar*=10 μm)

cells was lower than that observed in cells treated with c^3Ado, confirms our previous data suggesting c^3Ado plus Hcy initiates more potent apoptosis compared with c^3Ado. This is further supported by a more pronounced loss of intact DNA in cultures treated with c^3Ado plus Hcy. Fragmentation of the nucleus, organelle segregation and vesiculation was present in APC in both c^3Ado and c^3Ado plus Hcy treated cultures. Taken together these results may indicate that the qualitative difference between c^3Ado and c^3Ado plus Hcy apoptosis is restricted to the cytoplasmic membrane.

When compared with the c^3Ado and c^3Ado plus Hcy treated cultures, a higher chromatin/cytoplasm ratio and more uncondensed chromatin were evident in cultures exposed to c^3Ado plus CB. In addition, 66.0% of the DNA of control cells was intact after 12 h in cultures treated with c^3Ado plus CB, compared with 15.8% in c^3Ado treated cultures. These data suggest that the nuclear changes in apoptosis initiated by c^3Ado are partly inhibited by CB. Cytochalasins inhibit actin polymerization by capping the positive end of F-actin [10, 36]. Inhibited polymerization causes an increased concentration of actin monomers (G-actin) which are known inhibitors of DNase I [28, 44, 53]. Conflicting data exist concerning the nuclease responsible for internucleosomal DNA degradation in HL-60 apoptosis [5, 17, 38, 59], and G-actin sensitivity has so far not been demonstrated. Since CB but not CE inhibited c^3Ado apoptosis in the present study, it is not likely that elevated G-actin levels play a part in the mechanism by which CB inhibits c^3Ado apoptosis. The differential effect of CB and CE neither supports cytoskeleton alterations and subsequent changes of ion fluxes or perturbations of drug and/or effector molecule transport as important parts of the mechanism by which CB inhibits c^3Ado apoptosis. The opposite effect of CB and CE rather indicate that CB exerts its effect by an actin independent mechanism.

CB but not CE interact with glucose transport in mammalian cells [7, 45]. Energy dependency of the apoptotic process is demonstrated in several studies [29, 51]. The present data do not exclude that inhibition of glucose transport is one part of the mechanism by which CB inhibits apoptosis. However, we were not able to mimic the effect of CB on DNA degradation by 100 μM of another specific glucose transport inhibitor, phloretin (data not shown).

Cytochalasins are known to induce a transient increase in intracellular calcium due to release of calcium from intracellular stores [20, 52]. Interestingly, CB is far more potent than CE at increasing intracellular calcium levels [52]. With respect to apoptosis this effect is of particular interest since a drop of intracellular calcium may play a role in apoptosis initiation [3, 37, 55]. However, the role of intracellular calcium in initiation and progression of apoptosis in the HL-60 cell line is controversial [4, 35, 60]. One might speculate that the discrepancy between CB and CE observed herein could be due to different abilities between CB and CE to influence the intracellular calcium homeostasis during apoptosis initiation.

Cells without pseudopodial covering were observed in all treated cultures after 4 h, and the number of smooth surfaced cells reflected both the potency of c^3Ado and c^3Ado plus Hcy to initiate apoptosis and the inhibitory effect of CB. Smooth cells displayed either a blebbed or a non-blebbed phenotype, the blebbed phenotype being abundant in cultures exposed to c^3Ado. Blebbing most likely precedes the formation of APB during apoptosis. In the present study blebbing was reduced among APC in cultures treated with c^3Ado plus Hcy, supporting previous data on APB formation [14, 15], and non-existent among APC in cultures treated with c^3Ado plus CB. However, APC in c^3Ado plus Hcy and c^3Ado plus CB cultures demonstrated typical nuclear fragmentation, suggesting that different biochemical systems are involved in the nuclear and cellular fragmentation processes, respectively.

The mechanisms underlying the blebbing process are unknown. Elevated transglutaminase activity in APC has been associated with cross linking of cytoplasmic proteins to maintain cellular integrity during the formation of APB [18]. However, elevated activity of this enzyme does not explain blebbing per se. Furthermore, disruption of the cytoskeleton and actin-membrane interactions secondary to attack of calcium dependant proteases, calpains [19, 41, 43] alternatively oxygen and/or hydroxyl radicals [26], may cause cell surface blebbing. In the present study CB exposed cells exhibited polarization and often longer and broader pseudopoda when compared with control cells. These cells exhibited foci of strong FITC-phalloidin staining, a finding at odds with the extensive depolymerization of F-actin secondary to capping of the positive end by CB. This indicates that the main effect of CB on microfilaments in this cell line ōccurs at the level of microfilament organization and distribution [10, 47]. Cells with early apoptotic features in cultures treated with c^3Ado and CB often demonstrated foci of green fluorescence at the internal part of the cytoplasmic membrane, whereas blebbed APC were characterised by a total absence of F-actin. One possible interpretation of these data is that blebbing of the cytoplasmic membrane occurs in cells deficient of F-actin. This may be due to depolymerization of F-actin. Alternatively it may be due to degradation of F-actin by proteases [23, 24, 46] during progression of apoptosis. However, since the distribution of F-actin was not studied at the ultrastructural level we cannot exclude a role of actin polymerization and subsequent actin-myosin interactions in APC blebbing.

Like blebbed APC, non-blebbed APC in cultures treated with c^3Ado plus Hcy did not display green fluorescence. Since c^3Ado acts as both inhibitor and substrate of AdoHcyase the metabolic consequences of c^3Ado treatment are both Hcy depletion, build up of S-adenosylhomocysteine (AdoHcy) and formation of 3-deazaadenosylhomocysteine (c^3AdoHcy) [54]. Addition of Hcy favours formation of c^3AdoHcy [12, 13, 50, 61]. c^3AdoHcy is a potent inhibitor of transmethylation reactions and it has been claimed that phospholipid methyla-

tion alters the properties of the cytoplasmic membrane [27, 32]. A role for c^3AdoHcy in inhibition of the contractile response in guinea-pig lung parenchyma has been shown previously by Gieske et al. [21]. In contrast Stopford et al. [48] found no correlation between c^3AdoHcy levels and the ability of c^3Ado to disorganize microfilaments in macrophages. The F-actin observed in non-blebbed APC in c^3Ado plus CB cultures was not found in non-blebbed APC in cultures exposed to c^3Ado plus Hcy. This may reflect the fact that CB and c^3Ado plus Hcy interact with different targets within the cytoplasmic membrane; alternatively it reflects a difference in potency between CB and c^3Ado plus Hcy in their ability to interact with the actin cytoskeleton. An ongoing study in our laboratory demonstrates that large amounts of c^3AdoHcy are formed in HL-60 cells exposed to c^3Ado plus Hcy. More detailed studies are needed to rule out whether this metabolites ability to inhibit APC blebbing is due to effects on phospholipid methylation or interactions with cytoskeletal filaments.

In summary, we have shown the presence of blebbed and non-blebbed phenotypes of APC in HL-60 cultures treated with c^3Ado and c^3Ado plus Hcy. The differences among these phenotypes seem to be restricted to the cytoplasmic membrane. The deficiency of F-actin in blebbed APC questions the role of actin polymerization and actin-myosin interactions in the blebbing process of APC. CB delayed onset and partly inhibited c^3Ado apoptosis by an unknown mechanism.

Acknowledgements We thank Randi Olsen for skilled technical assistance. These studies were supported by grants from the Norwegian Cancer Society, the Norwegian Council for Science and the Humanities and the Erna and Olav Aakre Foundation.

References

1. Arends MJ, Wyllie AH (1991) Apoptosis: mechanisms and roles in pathology. Int Rev Exp Pathol 32:223–254
2. Arends MJ, Morris RG, Wyllie AH (1990) Apoptosis: the role of the endonuclease. Am J Pathol 136:593–608
3. Baffy G, Miyashita T, Williamson JR, Reed JC (1993) Apoptosis induced by withdrawal of interleukin-3 (IL-3) from an IL-3-dependent hematopoietic cell line is associated with repartitioning of intracellular calcium and is blocked by enforced bcl-2 oncoprotein production. J Biol Chem 268:6511–6519
4. Barry MA, Eastman A (1992) Endonuclease activation during apoptosis: the role of cytosolic Ca^{2+} and pH. Biochem Biophys Res Commun 186:782–789
5. Barry MA, Eastman A (1993) Identification of deoxyribonuclease II as an endonuclease involved in apoptosis. Arch Biochem Biophys 300:440–450
6. Bøe T, Gjertsen BT, Vintermyr OK, Houge G, Lanotte M, Døskeland SO (1991) The protein phosphatase inhibitor okadaic acid induces morphological changes typical of apoptosis in mammalian cells. Exp Cell Res 195:237–246
7. Carruthers A (1990) Faciliated diffusion of glucose. Physiol Rev 70:1135–1169
8. Chiang PK, Cantoni GL (1979) Perturbation of biochemical transmethylations by 3-deazaadenosine in vivo. Biochem Pharmacol 28:1897–1902
9. Cohen JJ (1993) Overview: mechanisms of apoptosis. Immunol Today 14:126–130
10. Cooper JA (1987) Effect of cytochalasin and phalloidin on actin. J Cell Biol 105:1473–1478
11. Cotter TG, Lennon SV, Glynn JM, Green DR (1992) Microfilament-disrupting agents prevent the formation of apoptotic bodies in tumor cells undergoing apoptosis. Cancer Res 52: 997–1005
12. Djurhuus R, Svardal AM, Ueland PM (1989) Differential effects on growth, homocysteine, and related compounds of two inhibitors of S-adenosylhomocysteine catabolism, 3-deazaadenosine and 3-deazaaristeromycin, in C3H/10T1/2 cells. Cancer Res 49:324–330
13. Duerre JA, Buttz HR, Ackerman JJ (1992) Effect of methylation inhibitors on gene expression in HL-60 cells. Biochem Cell Biol 70:703–711
14. Endresen PC, Eide TJ, Aarbakke J (1993) Cell death initiated by 3-deazaadenosine in HL-60 cells is apoptosis and is partially inhibited by homocysteine. Biochem Pharmacol 46:1893–1901
15. Endresen PC, Lysne S, Prytz PS, Aarbakke J (1994) Homocysteine increases the relative number of apoptotic cells and reduces the relative number of apoptotic bodies in HL-60 cells treated with 3-deazaadenosine. J Pharmacol Exp Ther 269:1245–1253
16. Eriksson JE, Goldman RD (1993) Protein phosphatase inhibitors alter cytoskeletal structure and cellular morphology. Adv Protein Phosphatases 7:335–357
17. Fernandes RS, Cotter TG (1993) Activation of a calcium magnesium independent endonuclease in human leukemic cell apoptosis. Anticancer Res 13:1253–1260
18. Fesus L (1993) Biochemical events in naturally occurring forms of cell death. FEBS Lett 328:1–5
19. Fox JEB, Austin CD, Reynolds CC, Steffen PK (1991) Evidence that agonist-induced activation of calpain causes shedding of procoagulant-containing microvesicles from the membrane of aggregating platelets. J Biol Chem 266:13289–13295
20. Garcia C, Montero M, Alvarez J, Crespo MS (1993) Biosynthesis of platelet-activating factor (PAF) induced by chemotactic peptide is modulated at the lyso-PAF:acetyl-CoA acetyltransferase level by calcium transient and phosphatidic acid. J Biol Chem 268:4001–4008
21. Gieske TH, Doherty NS, Raddatz R, Stephens D (1991) S-adenosylhomocysteine levels are not involved in the spasmolytic activity of 3-deazaadenosine in guinea-pig lung parenchyma. Pharmacology 42:151–155
22. Gjertsen BT, Cressey LI, Ruchaud S, Houge G, Lanotte M, Døskeland SO (1994) Multiple apoptotic death types triggered through activation of separate pathways by cAMP and inhibitors of protein phosphatases in one (IPC leukemia) cell line. J Cell Sci 12:3363–3377
23. Gong J, Li X, Darzynkiewicz Z (1993) Different patterns of apoptosis of HL-60 cells induced by cycloheximide and camptothecin. J Cell Physiol 157:263–270
24. Gorczyca W, Bruno S, Darzynkiewicz RJ, Gong J, Darzynkiewicz Z (1992) DNA strand breaks occurring during apoptosis: their early in situ detection by the terminal deoxynucleotidyl transferase and nick translation assays and prevention by serine protease inhibitors. Int J Oncol 1:639–648
25. Gundersen HJG, Bendtsen TF, Korbo L, Marcussen N, Møller A, Nielsen K et al. (1988) Some new, simple and efficient stereological methods and their use in pathological research and diagnosis. APMIS 96:379–394
26. Hinshaw DB, Sklar LA, Bohl B, Schraufstatter IU, Hyslop PA, Rossi MW et al. (1986) Cytoskeletal and morphologic impact of cellular oxidant injury. Am J Pathol 123:454–464
27. Hirata F, Axelrod J (1978) Enzymatic methylation of phosphatidylethanolamine increases membrane fluidity. Nature 275: 219–220
28. Kabsch W, Mannherz HG, Suck D, Pai EF, Holmes KC (1990) Atomic structure of the actin: DNase I complex. Nature 347: 37–44
29. Kaufmann SH (1989) Induction of endonucleolytic DNA cleavage in human acute myelogenous leukemia cells by etoposide, camptothecin, and other cytotoxic anticancer drugs: a cautionary note. Cancer Res 49:5870–5878

30. Kerr JFR, Harmon BV (1991) Definition and incidence of apoptosis: an historical perspective. In: Tomei LD, Cope FO (eds) Apoptosis: The molecular basis of cell death. (Current communications in cell and molecular biology, Vol 3) Cold Spring Harbor Laboratory Press, Cold Spring Harbor, pp 5–30
31. Kolber MA, Broschat KO, Landa-Gonzalez (1990) Cytochalasin B induces cellular DNA fragmentation. FASEB J 4: 3021–3027
32. Kuncl RW, Drachman DB, Adams R, Lehar M (1993) 3-Deazaadenosine: a therapeutic strategy for myasthenia gravis by decreasing the endocytosis of acetylcholine receptors. J Pharmacol Exp Ther 267:582–589
33. Larson RA, Yachnin S (1983) Cytochalasin B is a potent mitogen for chronic lymphocytic leukemia cells in vitro. J Clin Invest 72:1268–1276
34. Lazebnik YA, Cole S, Cooke CA, Nelson WG, Earnshaw WC (1993) Nuclear events of apoptosis in vitro in cell-free mitotic extracts: a model system for analysis of the active phase of apoptosis. J Cell Biol 123:7–22
35. Lennon SV, Kilfeather SA, Hallett MB, Campell AK, Cotter TG (1992) Elevations in cytosolic free Ca^{2+} are not required to trigger apoptosis in human leukaemia cells. Clin Exp Immunol 87:465–471
36. MacLean-Fletcher S, Pollard TD (1980) Mechanism of action of cytochalasin B on actin. Cell 20:329–341
37. Magnelli L, Cinelli M, Turchetti A, Chiarugi VP (1993) Apoptosis induction in 32D cells by IL-3 withdrawal is preceded by a drop in the intracellular calcium level. Biochem Biophys Res Commun 194:1394–1397
38. Matsubara K, Kubota M, Adachi S, Kuwakado K, Hirota H, Wakazono Y et al. (1994) Different mode of cell death induced by calcium ionophore in human leukemia cell lines: possible role of constitutive endonuclease. Exp Cell Res 210: 19–25
39. Matzinger P (1991) The JAM test: a simple assay for DNA fragmentation and cell death. J Immunol Methods 145:185–192
40. McDowell EM, Trumph BF (1976) Histologic fixatives suitable for diagnostic light and electron microscopy. Arch Pathol Lab Med 100:405–414
41. Nicotera P, Hartzell P, Davis G, Orrenius S (1986) The formation of plasma membrane blebs in hepatocytes exposed to agents that increase cytosolic Ca^{2+} is mediated by activation of a non-lysosomal proteolytic system. FEBS Lett 209:139–144
42. Oberhammer F, Fritsch G, Pavelka M, Froschl G, Tiefenbacher R, Purchio T et al. (1992) Induction of apoptosis in cultured hepatocytes and in the regressing liver by transforming growth factor-beta1 occurs without activation of an endonuclease. Toxical Lett 64/65:701–704
43. Orrenius S, McCabe MJ, Nicotera P (1992) Ca^{2+}-dependent mechanisms of cytotoxicity and programmed cell death. Toxical Lett 64/65:357–364
44. Peitsch MC, Polzar B, Stephan H, Crompton T, MacDonald HR, Mannherz HG et al. (1993) Characterization of the endogenous deoxyribonuclease involved in nuclear DNA degradation during apoptosis (programmed cell death). EMBO J 12: 371–377
45. Rampal AL, Pinkofsky HB, Jung CY (1980) Structure of cytochalasins and cytochalasin B binding site in human erythrocyte membranes. Biochemistry 19:679–683
46. Sarin A, Adams DH, Henkart PA (1993) Protease inhibitors selectively block T cell receptor-triggered programmed cell death in a murine T cell hybridoma and activated peripheral T cells. J Exp Med 178:1693–1700
47. Schilwa M (1982) Action of cytochalasin D on cytoskeletal networks. J Cell Biol 92:79–91
48. Stopford CR, Wolberg G, Prus KL, Reynolds-Vaughn R, Zimmerman TP (1985) 3-Deazaadenosine-induced disorganization of macrophage microfilaments. Proc Natl Acad Sci USA 82: 4060–4064
49. Sun DY, Jiang S, Zheng L-M, Ojcius DM, Young JD-E (1994) Separate metabolic pathways leading to DNA fragmentation and apoptotic chromatin condensation. J Exp Med 179:559–568
50. Svardal A, Djurhuus R, Ueland PM (1986) Disposition of homocysteine and S-3-deazaadenosylhomocysteine in cells exposed to 3-deazaadenosine. Mol Pharmacol 30:154–158
51. Thakkar NS, Potten CS (1993) Inhibition of doxorubicin-induced apoptosis in vivo by 2-deoxy-d-glucose. Cancer Res 53:2057–2060
52. Treves S, Di Virgilio F, Vaselli GM, Pozzan T (1987) Effect of cytochalasin on cytosolic-free calcium concentration and phosphoinositide metabolism in leukocytes. Exp Cell Res 168: 285–298
53. Ucker DS, Obermiller PS, Eckhart W, Apgar JR, Berger NA, Meyers J (1992) Genome digestion is a dispensable consequence of physiological cell death mediated by cytotoxic T lymphocytes. Mol Cell Biol 12:3060–3069
54. Ueland PM (1982) Pharmacological and biochemical aspects of S-adenosylhomocysteine and S-adenosylhomocysteine hydrolase. Pharmacol Rev 34:223–225
55. Whyte MKB, Hardwick SJ, Meagher LC, Savill JS, Haslett C (1993) Transient elevations of cytosolic free calcium retard subsequent apoptosis in neutrophils in vitro. J Clin Invest 92: 446–455
56. Wulf E, Deboben A, Bautz FA, Faulstich, Wieland TH (1979) Fluorescent phallotoxin, a tool for the visualization of cellular actin. Proc Natl Acad Sci USA 76:4498–4502
57. Wyllie AH, Kerr JF, Currie AR (1980) Cell death: the significance of apoptosis. Int Rev Cytol 68:251–306
58. Yahara I, Harada F, Sekita S, Yoshihira K, Natori S (1982) Correlation between effects of 24 different cytochalasins on cellular structures and cellular events and those on actin in vitro. J Cell Biol 92:69–78
59. Yoshida A, Ueda T, Wano Y, Nakamura T (1993) DNA damage and cell killing by camptothecin and its derivative in human leukemia HL-60 cells. Jpn J Cancer Res 84:566–573
60. Yoshida A, Ueda T, Takauji R, Liu Y-P, Fukushima T, Inuzuka M et al. (1993) Role of calcium in induction of apoptosis by etoposide in human leukemia HL-60 cells. Biochem Biophys Res Commun 196:927–934
61. Zimmerman TP, Iannone M, Wolberg G (1984) 3-Deazaadenosine: S-adenosylhomocysteine hydrolase-independent mechanism of action in mouse lymphocytes. J Biol Chem 259: 1122–1126